ChemPubSoc Europe

DOI: 10.1002/open.201500205

Open Access ChemistryOPEN Full Papers

Topological Control of Columnar Stacking Made of Liquid-Crystalline Thiophene-Fused Metallonaphthalocyanines

Hiroyuki Suzuki,[a] Koki Kawano,[b] Kazuchika Ohta,[a] Yo Shimizu,[b] Nagao Kobayashi,[a] and Mutsumi Kimura*[a]

The spontaneous organization of two-dimensional polyaromatic molecules into well-defined nanostructures through noncovalent interactions is important in the development of organic-based electronic and optoelectronic devices. Two regioisomers of thiophene-fused zinc naphthalocyanines **ZnTNc$_{endo}$** and **ZnTNc$_{exo}$** have been designed and synthesized to obtain photo- and electroactive liquid crystalline materials. Both compounds exhibited liquid crystalline behavior over a wide temperature range through intermolecular π–π interactions and local phase segregation between the aromatic cores and peripheral side chains. The structural differences between **ZnTNc$_{endo}$** and **ZnTNc$_{exo}$** affected the stacking mode in self-assembled columns, as well as symmetry of the two-dimensional rectangular columnar lattice. The columnar structure in liquid crystalline phase exhibited an ambipolar charge-transport behavior.

Introduction

Spontaneous organization of two-dimensional polyaromatic molecules into well-defined nanostructures through noncovalent interactions has been intensively explored, to realize organic-based electronic and optoelectronic devices.[1–3] The decoration of polyaromatic cores with flexible alkyl chains results in the formation of liquid-crystalline phases, which correspond to one-dimensional columnar stacks of polyaromatic molecules driven by the intermolecular π–π interactions and the local phase segregation between the flat rigid aromatic cores and peripheral side chains.[4,5] The intermolecular π–π overlap among polyaromatic molecules within the columns provides a transport pathway for charge or energy along the columnar axis. The charge carrier mobilities and semiconductivities can be tailored by designing polyaromatic cores and controlling the self-organization of molecules in the bulk.

Metallophthalocyanines (MPcs) and their analogs have been widely used as molecular materials in applications from organic pigments to semiconductors for electronic devices because of their unique optical properties and thermal stability.[6,7] Since the first report of liquid crystalline Pc by Piechocki and Simon[8], liquid crystalline MPcs have been modified to control the self-organized nanostructures, and applied as molecular components in organic thin-film transistors (OTFTs) and solar photovoltaics (OPVs).[9,10] The optical and electronic properties of MPcs strongly depend on the size of the π-system.[11] The expansion of the phthalocyanine π-system has been achieved by condensation of fused polyaromatic precursors.[12–18] The size and geometry of the annulated aromatic residues on the tetraazaporphyrin core affects the position of the Q band, as well as the HOMO and LUMO energy levels. Moreover, the expansion of the π-system enhances the tendency for π-stacking. Although various ring-expanded MPcs with alkyl chains have been synthesized, and their self-assembly properties in solution or on substrates investigated, there have been few reports on the spontaneous organization of liquid crystalline ring-expanded MPcs into nanostructures.[19–22]

In this paper, we report the syntheses of two isomeric, thiophene-fused zinc naphthalocyanines (Nc), **ZnTNc$_{endo}$** and **ZnTNc$_{exo}$**, decorated with sixteen dodecyl chains, and their self-organization properties. Thiophene-fused polyaromatic molecules display excellent performance in OTFT and OPV, due to the formation of three-dimensional molecular stacks through sulfur–sulfur contact between thiophene segments.[23,24] We hoped to control the organized structure of ring-expanded MPcs and enhance the charge mobilities by fusing with thiophene rings at the peripheral positions of the Nc ring. The physical properties and self-organized structures in the liquid crystalline phase, and the carrier mobilities of the two isomers were compared with each other.

[a] *H. Suzuki, Prof. K. Ohta, Prof. N. Kobayashi, Prof. M. Kimura*
Division of Chemistry and Materials
Faculty of Textile Science and Technology
Shinshu University, Ueda 386-8567 (Japan)
E-mail: mkimura@shinshu-u.ac.jp

[b] *K. Kawano, Dr. Y. Shimizu*
National Institute of Advanced Industrial Science and Technology
Kansai-Center, 1-8-31 Midorigaoka, Ikeda, Osaka 563-8577 (Japan)

Supporting information for this article is available on the WWW under http://dx.doi.org/10.1002/open.201500205.

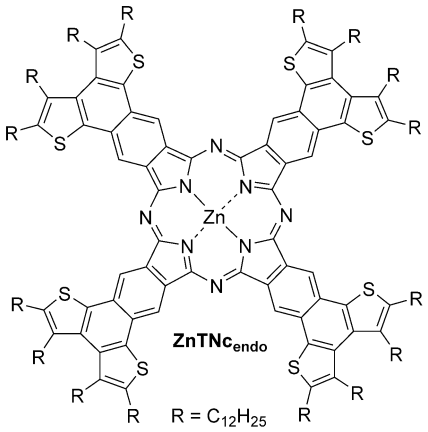

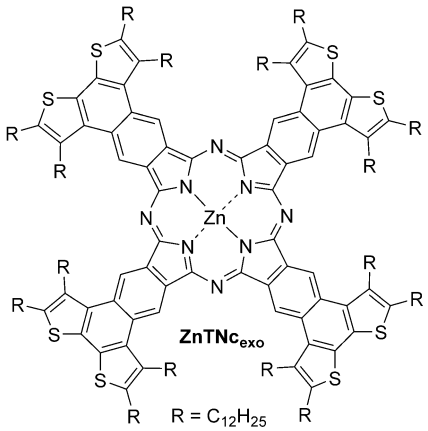

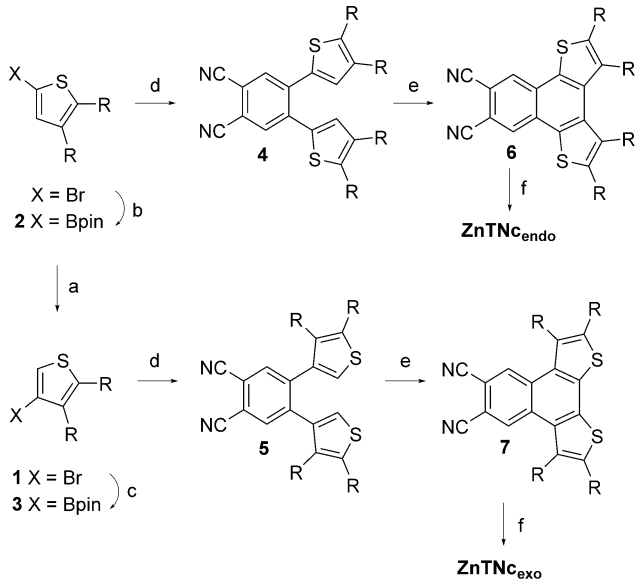

Scheme 1. Syntheses of ZnTNc$_{endo}$ and ZnTNc$_{exo}$. *Reagents and conditions*: a) LDA, THF, rt, 12 h, 80%; b) i) 1.6 M *n*BuLi, THF, −78 °C, 1 h; ii) 2-isopropoxy-4,4,5,5-tetramethyl- 1.3.2-dioxaborolane, rt, 12 h, 72%; c) bis(pinacolato)diboron, Pd(dppf)Cl_2·CH_2Cl_2, KOAc, 1,4-dioxane, 80 °C, 6 h, 44%; d) 4,5-dichlorophthalonitrile, $Pd(OAc)_2$, S-Phos, K_3PO_4, toluene, DME, H_2O, 85 °C, 12 h, 61%; e) $FeCl_3$, CH_3NO_2, CH_2Cl_2, 0 °C, 0.5 h, 86%; f) $Zn(OAc)_2$, DBU, 1-pentanol, 140 °C, 12 h, 50%.

Results and Discussion

Thiophene-fused ZnNc derivatives were synthesized from 4,5-dithienylphthalonitrile by Yan et al., and they studied their aggregation behavior in solution.[25] In this paper, we designed and synthesized two isomers, **ZnTNc$_{endo}$** and **ZnTNc$_{exo}$**, possessing sixteen dodecyl chains, in which flexible dodecyl chains were attached to the two positions of the peripheral thiophene rings.

Regioisomers of thiophene-fused phthalonitriles **6** and **7** were synthesized from 2-bromo-4,5-didodecylthiophene as a starting material (Scheme 1). 2-Bromo-4,5-didodecylthiophene was prepared from 3-bromothiophene according to the procedure reported by Kuo et al.[26] Compound **2** was synthesized from 2-bromo-4,5-didodecylthiophene by the selective lithiation at the α-hydrogen of the thiophene ring using *n*-butyllithium, followed by reaction with 2-isopropoxy-4,4,5,5-tetramethyl-1,3,2-dioxaborolane.[27] The other isomer **3** was prepared in two synthetic steps: isomerization of 2-bromo-4,5-didodecylthiophene with lithium diisopropylamide (LDA),[28,29] and the palladium-catalyzed Miyaura borylation reaction with bis(pinacolato)diboron.[30,31] Phthalonitrile precursors **4** and **5** were synthesized by the Suzuki–Miyaura coupling reaction of 4,5-dichlorophthalonitrile with **2** or **3** in the presence of a palladium catalyst using S-Phos ligand.[32] The two thiophenes in **4** and **5** were fused by $FeCl_3$-mediated oxidative cyclization.[28,29] Phthalonitriles **6** and **7**, in which two thiophenes are annealed at different positions, were isolated as yellow solids, and unambiguously characterized by NMR spectroscopy, FT-IR, and matrix-asssited laser desorption ionization–time-of-flight mass spectrometry (MALDI-TOF MS).

Figure 1a shows the absorption and fluorescence spectra of **6** and **7** in CH_2Cl_2. The shapes of the absorption spectra of **6** and **7** were different, and the emission maximum of **7** was red-shifted relative to that of **6**. Density functional theory (DFT) calculations were conducted for **6** and **7**, in order to gain insight into the equilibrium geometries and electronic structures of the frontier orbitals of the compounds. The transitions calculated by time-dependent (TD) DFT agreed well with the experimental absorption spectra of **6** and **7** (Figure S3). While **7** has a planar geometry, the other isomer **6** shows a less planar structure as shown in Figure 1b. The steric hindrance arising from the methyl units of two different thiophenes in **7** induces strain in the thiophene-fused phthalonitrile. The differences in the absorption and fluorescence spectra of **6** and **7** can be explained by a change in conjugation caused by the strain of the aromatic rings.[33]

The syntheses of **ZnTNc$_{endo}$** and **ZnTNc$_{exo}$** decorated with sixteen alkyl chains were achieved by heating **6** or **7** with 1,8 diazabicyclo[5.4.0]undec-7-ene (DBU) and zinc acetate in *n*-pentanol.[34,35] Both complexes were characterized by NMR spectroscopy and MALDI-TOF MS, and were found to be highly soluble in many organic solvents except for acetone and alcohols. Phthalocyanine analogs exhibit a strong absorption band (Q band) in the near-infrared (IR) region, and the Q band position can be shifted to longer wavelengths with increasing size of the π-system.[11] However, **ZnTNc$_{endo}$** and **ZnTNc$_{exo}$** showed

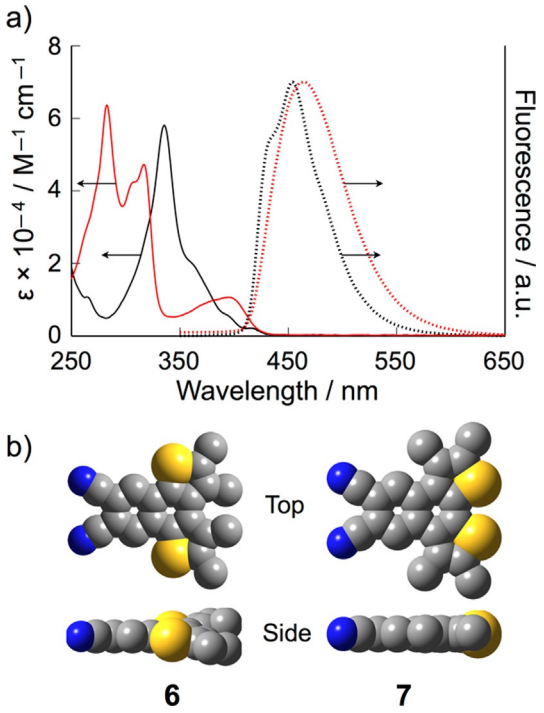

Figure 1. a) Absorption and fluorescence spectra of **6** (black line) and **7** (red line) in CH_2Cl_2. b) Optimized structures of **6** and **7** (methyl-substituted analogs) obtained by DFT at the B3LYP/6-31G(d) level.

sharp Q bands at 775 and 778 nm in tetrahydrofuran (THF, Figure 2a and Table 1), and the positions of the Q band in **ZnTNc$_{endo}$** and **ZnTNc$_{exo}$** are equal to that of zinc(II) tetra(*tert*-butyl)naphthalocyanine (Zn(*t*Bu)Nc) lacking fused thiophene rings (λ_{max} = 778 nm).[36] The fluorescence spectra of **ZnTNc$_{endo}$** and **ZnTNc$_{exo}$** have a peak at 783 nm with a near mirror image of the Q band and a very small Stoke-shift. The optical HOMO–LUMO band gaps (E_g) for **ZnTNc$_{endo}$** and **ZnTNc$_{exo}$** were determined to be 1.6 eV from the crossing point of the normalized absorption and fluorescence spectra. The electron density distributions of the HOMO and LUMO calculated by DFT are mainly populated over the Nc skeleton within **ZnTNc$_{endo}$** and **ZnTNc$_{exo}$** (Figure 2b and S4). While the Q band position of phthalocyanine can be shifted to the near-IR by linear annulation, to form Nc and further to further anthracocyanine, the angular annulation does not result in a red-shift of the Q band.[11,37] The fusing of thiophene rings at the angular positions of Nc in **ZnTNc$_{endo}$** and **ZnTNc$_{exo}$** does not effect a shift of the Q band as well as the change of E_g.

Table 1. Photochemical, electrochemical, and thermal analysis data of **ZnTNc$_{endo}$** and **ZnTNc$_{exo}$**.

	λ_{abs}[a] [nm]	$\varepsilon_{max}\times10^{-5}$ [$M^{-1}cm^{-1}$]	λ_{fl}[a] [nm]	E_g^{opt}[b] [eV]	HOMO[c] [eV]	LUMO[c] [eV]	T (ΔH)[d] [°C (kJ mol^{-1})]	T_d[e] [°C]
ZnTNc$_{endo}$	775	3.72	783	1.6	−4.8	−3.2	−5.5 (8), 257 (6)	259
ZnTNc$_{exo}$	778	3.55	782	1.6	−4.7	−3.1	5.1 (16), 204 (12)	245

[a] Measured in THF. [b] Estimated from cross point of normalized absorption and fluorescence spectra. [c] HOMO and LUMO energy levels were determined by HOMO = −(4.8 + $E_{ox}^{1/2}$ (vs. Fc/Fc$^+$) and LUMO = HOMO + E_g^{opt}. [d] Phase transition temperatures and their enthalpies determined by differential scanning calorimetry (DSC). [e] Temperature of starting weight loss determined by thermogravimetric analysis (TGA).

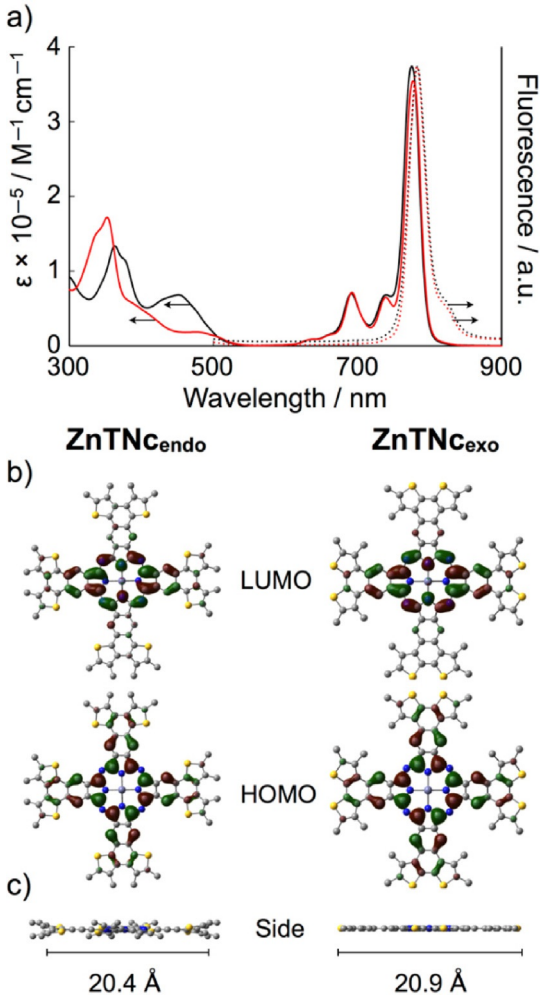

Figure 2. a) Absorption and fluorescence spectra of **ZnTNc$_{endo}$** (black line) and **ZnTNc$_{exo}$** (red line) in THF. b,c) HOMO/LUMO orbitals and optimized structures of **ZnTNc$_{endo}$** and **ZnTNc$_{exo}$** (methyl-substituted analogs) obtained by DFT at the B3LYP/6-31G(d) level.

According to the equilibrium geometries calculated by DFT (Figure 2c), the peripheral two thiophene rings in **ZnTNc$_{endo}$** are twisted, due to the steric repulsion of neighboring alkyl groups. The molecular dimensions of **ZnTNc$_{endo}$** and **ZnTNc$_{exo}$** were estimated from the analysis of the surface pressure versus area (π–A) isotherm on pure water as the subphase (Figure S5 in the Supporting Information).[38] The limiting surface areas per molecule of **ZnTNc$_{endo}$** and **ZnTNc$_{exo}$** were estimated to be 1.47 and 1.10 nm^2, respectively, determined by extrapolating the slope of the π–A isotherm in the liquid-condensed region to zero pressure. The observed area of **ZnTNc$_{endo}$** was larger than that of **ZnTNc$_{exo}$**, suggesting a larger stacking distance between the thiophene-fused Nc

rings within the edge-on stacks on water by distortion of the structure from planarity in **ZnTNc$_{endo}$**.

The HOMO energy levels of **ZnTNc$_{endo}$** and **ZnTNc$_{exo}$** were determined from the first oxidation potential (E_{ox}) by differential pulse voltammetry measurements in dry dichloromethane containing 0.1 M nBu$_4$NClO$_4$ as a supporting electrolyte. Both complexes exhibited one oxidation peak for the oxidation of the naphthalocyanine ring (ZnNc(−1)/ZnNc(−2)) at −0.02 and −0.15 V vs. the ferrocene/ferrocenium couple (Fc/Fc^+), which were negative relative to the E_{ox} of Zn(*t*Bu)Nc (Table 1).[36] The HOMO energy levels of **ZnTNc$_{endo}$** and **ZnTNc$_{exo}$** were estimated to be −4.8 and −4.7 eV, respectively, from E_{ox} calibrated by the Fc/Fc^+ redox potential vs. vacuum. The HOMO and LUMO energy levels of **ZnTNc$_{endo}$** and **ZnTNc$_{exo}$** were higher than those of Zn(*t*Bu)Nc, indicating that the fusing of thiophene rings with the Nc ring leads to the destabilization of HOMO and LUMO energy levels.[36]

The thermal phase transition behavior of **ZnTNc$_{endo}$** and **ZnTNc$_{exo}$** was investigated by a combination of differential scanning calorimetry (DSC) and temperature-controlled polarizing optical microscopy (TPOM). The DSC profile of **ZnTNc$_{exo}$** showed two reversible transitions at 5 and 204 °C upon heating (Table 1). In thermogravimetric analysis (TGA) curves, **ZnTNc$_{exo}$** exhibited an onset of weight loss above 240 °C, suggesting that decomposition does not occur at the transition point, as observed in the DSC. Under TPOM, a birefringent dendritic texture appeared at 190 °C on cooling from the isotropic melt, and remained without any change until room temperature (Figure 3a). This texture is typical of columnar liquid crystalline materials.[39,40] To confirm the self-organized structure of **ZnTNc$_{exo}$** in the liquid crystalline state, temperature-controlled X-ray diffraction (XRD) measurements were performed. The XRD profile of **ZnTNc$_{exo}$** at 100 °C revealed a set of diffraction peaks corresponding to a d spacing of 30.0, 24.5, 12.5, 10.1, and 8.46 Å, which were indexed in sequence as (100), (200), (320), (330), and (340) of a rectangular columnar (Col$_r$) lattice with lattice parameters of a = 49.0 and b = 38.7 Å, and with the number of molecules in the unit cell Z = 2. The rectangular lattice has a $P2_1/a$ symmetry, as shown in Figure 4a. Moreover, the XRD profile in the wide-angle region showed only a broad halo around d = 4.6 Å, and did not exhibit reflections corresponding to the stacking periodicity in the columnar assemblies. While the other isomer **ZnTNc$_{endo}$** also exhibited a columnar liquid crystalline phase, the transition temperature of **ZnTNc$_{endo}$** from the liquid crystalline state to the isotropic melt was 53 °C higher than that of **ZnTNc$_{exo}$**. The texture of **ZnTNc$_{endo}$** in the liquid crystalline state under TPOM was also different from **ZnTNc$_{exo}$** (Figure 3b). The XRD reflections of **ZnTNc$_{endo}$** were fitted to a two-dimensional Col$_r$ lattice with $P2m$ symmetry (Figure 4b and S6 in the Supporting Information).

Figure 3c shows UV/Vis spectra of thin films of **ZnTNc$_{exo}$** and **ZnTNc$_{endo}$** in the liquid crystalline state on quartz plates. UV/Vis spectra provide information on the type of aggregated structures, such as face-to-face, edge-to-edge, and herringbone arrangements.[41,42] The maximum of the Q band for the film of **ZnTNc$_{endo}$** in the liquid crystalline phase was found to be

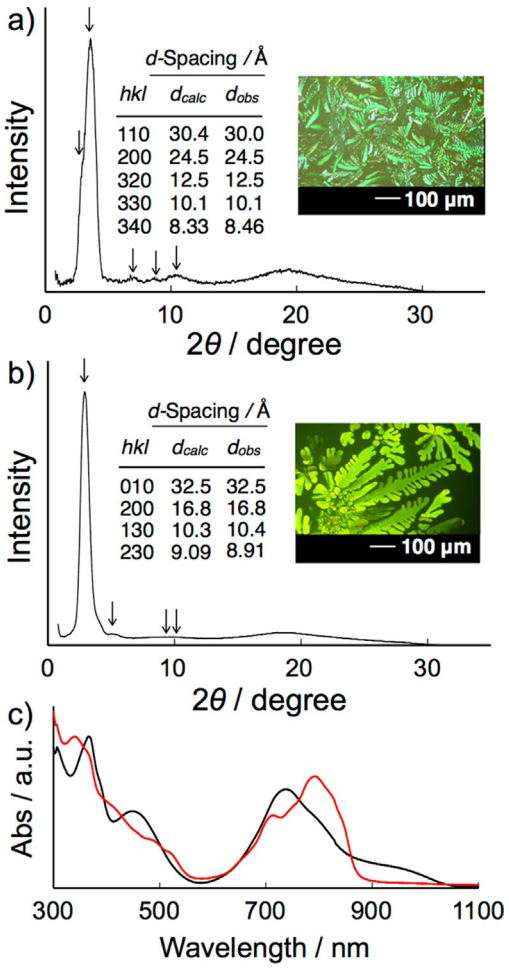

Figure 3. X-ray diffraction (XRD) patterns of a) **ZnTNc$_{exo}$** at 100 °C and b) **ZnTNc$_{endo}$** at 160 °C. The insets show crossed polarized optical micrographs of **ZnTNc$_{exo}$** at 190 °C and **ZnTNc$_{endo}$** at 240 °C, and d-spacing values for **ZnTNc$_{exo}$** and **ZnTNc$_{endo}$**. c) Absorption spectra of **ZnTNc$_{endo}$** (black line) and **ZnTNc$_{exo}$** (red line) in their liquid crystalline states on quartz plates.

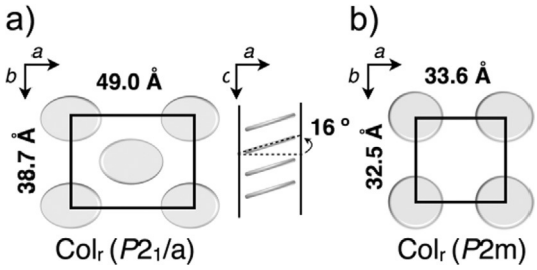

Figure 4. Schematic illustrations of two-dimensional columnar packing symmetry and one-dimensional molecular stacking feature of a) **ZnTNc$_{exo}$** and b) **ZnTNc$_{endo}$**.

737 nm, and the blue shift of the Q band compared with the solution spectrum indicates the formation of stacks having a face-to-face arrangement. On the other hand, the **ZnTNc$_{exo}$** film showed a red shift of the Q band position relative to the solution spectrum, suggesting that the aromatic planes in **ZnTNc$_{endo}$** were stacked in an eclipsed conformation within the one-dimensional stacks (Figure 4a). The tilted angle of the aromatic plane of **ZnTNc$_{exo}$** in the stacks was estimated to be 16 degrees from the horizontal axis, based on the lattice pa-

rameters in the XRD analysis and the molecular dimensions from the DFT calculations. Liquid crystalline Pc and benzoporphyrins substituted with alkyl chains at the lateral positions also showed an eclipsed conformation with a tilt angle to the columnar axis.[43–45] The lateral alkyl chains located at the crowded bay areas of **ZnTNc$_{exo}$** reduce the strength of intermolecular interactions between the aromatic cores due to the steric repulsion of alkyl chains arranged out of the core plane. Recently, Aida and coworkers reported liquid crystalline behavior of propeller-shaped fused oligothiophenes.[29] They found the formation of long-range columnar assemblies of oligothiophenes through well-organized intermolecular sulfur–sulfur contacts. The transition enthalpy of **ZnTNc$_{exo}$** from the Col$_r$ to the isotropic phase was larger than that of **ZnTNc$_{endo}$**. The peripheral sulfur atoms in **ZnTNc$_{exo}$** can interact with the other molecules in the neighboring column, and the sulfur–sulfur interaction may stabilize the intercolumnar assemblies in the Col$_r$ phase. However, we do not have data to support the formation of intermolecular sulfur–sulfur interactions at this stage.

The well-organized columnar nanostructures made from liquid crystalline π-conjugated polyaromatic materials can create long-range pathways for mobile charge carriers.[46] The carrier mobilities of liquid crystalline materials have been measured by time-of-flight (TOF) and radiolysis-time resolved microwave conductivity.[47–50] The TOF method gives mobilities of more than micrometer-scale distance in bulk materials. To evaluate the mobilities of **ZnTNc$_{exo}$** and **ZnTNc$_{endo}$**, TOF measurements were performed for **ZnTNc$_{exo}$** and **ZnTNc$_{endo}$** in the liquid crystalline states. Since the onset of the thermal decomposition of **ZnTNc$_{endo}$** is very close to the melting point, the carrier mobility μ of **ZnTNc$_{endo}$** could not be obtained because of the decomposition during the preparation of measurement cell. In contrast, the other isomer **ZnTNc$_{exo}$** showed transient photocurrents in the Col$_r$ phase of **ZnTNc$_{exo}$** at 50 and 150 °C under different applied biases at ±65 and ±80 V. Compound **ZnTNc$_{exo}$** exhibited an ambipolar carrier transport behavior (Figure S7 in the Supporting Information). The hole and electron mobilities are calculated to be 7×10^{-2} and 8×10^{-2} cm^{2}V^{-1}s^{-1}, and the mobilities are independent of electrical field as well as temperature. Because **ZnTNc$_{exo}$** formed multidomains with imperfect alignment of columns between two electrodes, the hole and electron mobilities of **ZnTNc$_{exo}$** are slightly lower than the reported values of liquid crystalline Pcs.[51]

In conclusion, we have designed and synthesized two structural regioisomers of near-IR light-absorbing **ZnTNc$_{exo}$** and **ZnTNc$_{endo}$** decorated with sixteen long alkyl chains. We have elucidated the influence of the molecular structural differences in the two isomers on their self-organizing behavior and photoconductivity. Ring-expanded **ZnTNc$_{exo}$** and **ZnTNc$_{endo}$** assemble into one-dimensional columnar nanostructures over a wide temperature range from room temperature. TOF experiments have revealed that the organized **ZnTNc$_{exo}$** shows a well-balanced ambipolar carrier transport behavior, with carrier mobilities of the order of 10^{-2} cm^{2}V^{-1}s^{-1}. Spontaneous alignment of columnar assemblies on substrates is a key issue for improving the carrier mobilities. Work is underway in our laboratory to control the columnar alignment on the substrate by structural elaboration of thiophene-fused naphthalocyanines.

Experimental Section

General procedures

NMR spectra were recorded on a Bruker AVANCE 400 FT NMR spectrometer (Billerica, MA, USA) at 399.65 MHz and 100.62 MHz for ^{1}H and ^{13}C in $CDCl_3$ solution. Chemical shifts are reported relative to internal tetramethylsilane (TMS). IR spectra were obtained on a SHIMAZU IR Prestige-21 with DuraSample IR II (Kyoto, Japan). Absorption spectra were measured on a SHIMAZU UV-2600. MALDI-TOF mass spectra were obtained on a Bruker Autoflex spectrometer with dithranol as matrix.

All chemicals were purchased from commercial suppliers and used without further purification. 2-Bromo-4,5-didodecylthiophene was synthesized according to the literature method.[26] Column chromatography was performed with activated alumina (Wako, 200 mesh) or silica gel (Wakogel C-200). Recycling preparative gel permeation chromatography was carried out by a JAI recycling preparative HPLC using $CHCl_3$ as an eluent. Analytical thin layer chromatography was performed with commercial Merck plates coated with silica gel 60 F_{254} or aluminum oxide 60 F_{254}.

Syntheses

Replacement of substitution position[28,29]

3-Bromo-4,5-didodecylthiophene (1): To a solution of diisopropylamine (1.43 mL, 10.2 mmol) in THF (60 mL) was slowly added *n*-BuLi (1.6 M in hexanes, 4.5 mL, 7.20 mmol), and the reaction kept for 30 min at 0 °C under an Ar atmosphere. A solution of 2-bromo-4,5-didodecylthiophene (3.0 g, 6.00 mmol) in THF (15 mL) was added, and the mixture stirred for 12 h at rt, then the reaction mixture poured into H_2O and extracted with *n*-hexane. The organic layer was washed with saturated aqueous NH_4Cl (3×100 mL) and H_2O (3×100 mL), and dried over Na_2SO_4. The residue was purified by column chromatography on silica gel by eluting with *n*-hexane, to give **1** as a colorless liquid (2.41 g, 80%); ^{1}H NMR ($CDCl_3$, 400.13 MHz): δ = 6.95 (1H, s, Ar*H*), 2.72 (2H, t, J = 7.2 Hz, CH_2), 2.53 (2H, t, J = 7.6 Hz, CH_2), 1.57–1.65 (2H, m, CH_2), 1.45–1.52 (2H, m, CH_2), 1.26–1.32 (36H, m, CH_2), 0.88 ppm (6H, t, J = 6.4 Hz, CH_3); ^{13}C NMR ($CDCl_3$, 100.61 MHz): δ = 140.2, 136.7, 119.1, 112.9, 32.5, 32.1, 30.5, 30.3, 30.2, 30.1, 30.0, 29.9, 29.4, 28.4, 23.3, 14.6 ppm.

Attachment of borate ester

2-(4,4,5,5-Tetramethyl-1,3,2-dioxaborolan-2-yl)-4,5-didodecylthiophene (2):[26] To a solution of 2-bromo-4,5-didodecylthiophene (4.0 g, 8.01 mmol) in THF (100 mL) was added dropwise *n*-BuLi (1.6 M in hexanes, 6.0 mL, 9.61 mmol) at −78 °C under an Ar atmosphere, and the mixture stirred for 1 h at the same temperature under an Ar atmosphere. To this reaction mixture was slowly added 2-isopropoxy-4,4,5,5-tetramethyl-1,3,2-dioxaborolane (1.79 g, 9.62 mmol), and the reaction mixture stirred o/n at rt. The reaction was quenched by adding a small amount of MeOH and ether added to the mixture. The organic layer was washed with brine (3×100 mL), H_2O (3×100 mL), dried over Na_2SO_4, and the solvent evaporated. The residue was purified by column chromatography on silica gel by eluting with EtOAc/*n*-hexane (1:10 *v*/*v*), to give **2** as

a colorless liquid (3.17 g, 72%); ^{1}H NMR ($CDCl_3$, 400.13 MHz): δ = 7.37 (1H, s, Ar*H*), 2.73 (2H, t, J = 7.2 Hz, CH_2), 2.49 (2H, t, J = 7.6 Hz, CH_2), 1.54–1.66 (4H, m, CH_2), 1.26–1.41 (36H, m, CH_2), 1.23 (12H, s, CH_3), 0.88 ppm (6H, t, J = 6.4 Hz, CH_3); ^{13}C NMR ($CDCl_3$, 100.61 MHz): δ = 147.5, 140.0, 139.6, 84.1, 32.4, 32.1, 31.2, 30.2, 30.1, 30.0, 29.9, 29.8, 29.7, 28.6, 28.5, 25.2, 25.1, 23.2, 14.5 ppm.

3-(4,4,5,5-Tetramethyl-1,3,2-dioxaborolan-2-yl)-4,5-didodecylthiophene (3):[30,31] To a solution of **1** (1.0 g, 2.00 mmol) in 1,4-dioxane (10 mL) were added bis(pinacolato)diboron (0.762 g, 3.00 mmol), [1,1′-bis(diphenylphosphino)ferrocene]dichloropalladium(II), complex with dichloromethane [Pd(dppf)Cl_2·CH_2Cl_2] (0.163 g, 0.200 mmol), and KOAc (0.589 g, 6.00 mmol). The reaction mixture was stirred at 80 °C for 6 h under an Ar atmosphere, then the reaction quenched by adding H_2O, and extracted with ether (3× 50 mL). The organic layer was washed with brine (3×100 mL) and H_2O (3×100 mL), dried over Na_2SO_4, and the solvent evaporated. The residue was purified by column chromatography on silica gel by eluting with EtOAc/*n*-hexane (1:3 *v*/*v*), to give **3** as a colorless liquid (0.480 g, 44%); ^{1}H NMR ($CDCl_3$, 400.13 MHz): δ = 7.65 (1H, s, Ar*H*), 2.69–2.74 (4H, m, CH_2), 1.58–1.65 (2H, m, CH_2), 1.42–1.50 (2H, m, CH_2), 1.29 (12H, s, CH_3), 1.27–1.37 (36H, m, CH_2), 0.88 ppm (6H, t, J = 6.4 Hz, CH_3); ^{13}C NMR ($CDCl_3$, 100.61 MHz): δ = 143.3, 140.0, 134.3, 83.4, 32.6, 32.4, 32.1, 30.3, 30.2, 30.1, 29.9, 29.8, 28.5, 28.5, 28.1, 25.2, 23.2, 14.6 ppm.

Suzuki–Miyaura coupling reaction[32]

1,2-Dicyano-4,5-bis(4,5-didodecyl-2-thienyl)benzene (4): To a solution of 4,5-dichlorophthalonitrile (90.1 mg, 0.457 mmol) and **2** (1.00 g, 1.83 mmol) in a mixed solvent of toluene (2.0 mL), 1,2-dimethoxyethane (DME, 2.0 mL) and H_2O (1.0 mL) were added $Pd(OAc)_2$ (1.03 mg, 4.59 μmol), 2-dicyclohexylphosphino-2′,6′-dimethoxybiphenyl (S-Phos) (3.75 mg, 9.13 μmol) and K_3PO_4(0.397 g, 1.83 mmol), and the reaction mixture stirred at 85 °C for 12 h under an Ar atmosphere. After cooling to rt, the reaction mixture was poured into H_2O (50 mL), and extracted with CH_2Cl_2 (3× 30 mL). The organic layer was dried over $MgSO_4$, and the solvent evaporated. The residue was purified by column chromatography on silica gel by eluting with CH_2Cl_2/*n*-hexane (1:1 *v*/*v*) and recycling preparative HPLC, to give **4** as a pale yellow oily liquid (0.269 g, 61%); ^{1}H NMR ($CDCl_3$, 400.13 MHz): δ = 7.81 (2H, s, Ar*H*), 6.72 (2H, s, Ar*H*), 2.69 (4H, t, J = 7.6 Hz, CH_2), 2.43 (4H, t, J = 7.2 Hz, CH_2), 1.55–1.63 (4H, m, CH_2), 1.44–1.49 (4H, m, CH_2), 1.26–1.33 (72H, m, CH_2), 0.88 ppm (12H, t, J = 6.8 Hz, CH_3); ^{13}C NMR ($CDCl_3$, 100.61 MHz): δ 143.6, 139.4, 139.3, 135.5, 134.2, 131.2, 115.8, 113.6, 32.6, 32.2, 31.2, 30.2, 30.1, 30.0, 29.9, 29.8, 29.7, 28.5, 28.3, 23.1, 14.5 ppm.

1,2-Dicyano-4,5-bis(4,5-didodecyl-3-thienyl)benzene (5): Compound **5** was synthesized from 4,5-dichlorophthalonitrile (66.1 mg, 0.335 mmol) and **3** (0.737 g, 1.35 mmol) by the same procedure as for **4**, affording a yellow oily liquid (217 mg, 67%); ^{1}H NMR ($CDCl_3$, 400.13 MHz): δ = 7.75 (2H, s, Ar*H*), 6.68 (2H, s, Ar*H*), 2.67 (4H, t, J = 7.6 Hz, CH_2), 2.18 (4H, t, J = 6.4 Hz, CH_2), 1.58 (4H, t, J = 7.2 Hz, CH_2), 1.26–1.37 (76H, m, CH_2), 0.879 ppm (12H, t, J = 7.2 Hz, CH_3); ^{13}C NMR ($CDCl_3$, 100.61 MHz, ppm): δ = 143.4, 141.5, 138.4, 136.1, 135.6, 122.6, 115.8, 114.1, 32.4, 32.2, 31.0, 30.1, 30.0, 29.9, 29.8, 29.7, 29.6, 29.4, 28.7, 27.3, 23.1, 21.7, 14.5 ppm.

$FeCl_3$-mediated oxidative cyclization[28,29]

8,9-Dicyano-2,3,4,5-tetradodecyl-naphtho[1,2-*b*:4,3-*b*′]dithiophene (6): To a CH_2Cl_2 solution (50 mL) of **4** (0.269 g, 0.307 mmol) was added a CH_3NO_2 solution (10 mL) of $FeCl_3$ (0.226 g, 1.39 mmol) at 0 °C under an Ar atmosphere, and the resulting solution stirred at rt for 30 min. The reaction was quenched by adding MeOH (25 mL), and an organic extract washed with brine (3×50 mL) and saturated aqueous NH_4Cl (3×50 mL), dried over Na_2SO_4, and the solvent evaporated. The residue was purified by column chromatography on silica gel by eluting with CH_2Cl_2/*n*-hexane (1:1 *v*/*v*) and recrystallization from acetone, to give **6** as a pale yellow solid (0.193 g, 72%); mp: 53 °C; ^{1}H NMR ($CDCl_3$, 400.13 MHz): δ = 8.42 (2H, s, Ar*H*), 2.97–3.05 (8H, m, CH_2), 1.75–1.82 (4H, m, CH_2), 1.17–1.46 (76H, m, CH_2), 0.85–0.89 ppm (12H, m, CH_3); ^{13}C NMR ($CDCl_3$, 100.61 MHz): δ = 144.5, 137.5, 136.2, 133.8, 130.8, 127.7, 116.6, 109.6, 32.4, 32.0, 30.4, 30.2, 30.1, 30.0, 29.9, 29.8, 29.7, 23.1, 14.5 ppm;. IR (ATR): $\tilde{\nu}$ = 2228 cm^{-1} (CN); UV/Vis (CH_2Cl_2): λ (log ε/$M^{-1}cm^{-1}$) = 336 nm (4.76); MALDI-TOF MS (dithranol) *m*/*z* $[M+H]^+$ calcd for $C_{64}H_{102}N_2S_2$: 962.75, found: 962.08.

5,6-Dicyano-2,3,8,9-tetradodecyl-naphtho[2,1-*b*:3,4-*b*′]dithiophene (7): Compound **7** was synthesized from **5** (0.216 g, 0.224 mmol) and $FeCl_3$ (0.181 g, 1.12 mmol) by the same procedure as for **6** to yield a pale yellow solid (0.185 g, 86%); mp: 57 °C; ^{1}H NMR ($CDCl_3$, 400.13 MHz): δ = 8.78 (2H, s, Ar*H*), 3.03 (4H, t, J = 6.8 Hz, CH_2), 2.93 (4H, t, J = 7.6 Hz, CH_2), 1.73–1.81 (4H, m, CH_2), 1.26–1.67 (76H, m, CH_2), 0.878 ppm (12H, t, J = 7.2 Hz, CH_3); ^{13}C NMR ($CDCl_3$, 100.61 MHz): δ = 141.6, 136.2, 134.6, 131.0, 130.5, 129.6, 116.9, 108.6, 32.4, 30.1, 30.0, 29.9, 29.8, 29.7, 29.4, 29.2, 23.1, 14.5 ppm; IR (ATR): $\tilde{\nu}$ = 2228 cm^{-1} (CN); UV/Vis (in CH_2Cl_2): λ (log ε/$M^{-1}cm^{-1}$) = 285 (4.80), 317 (4.67), 395 nm (4.03); MALDI-TOF MS (dithranol) *m*/*z* $[M+H]^+$ calcd for $C_{64}H_{102}N_2S_2$: 962.75, found: 962.28.

Teteracyclization of 6 and 7[34,35]

ZnTNc$_{endo}$: A mixture of **6** (100.0 mg, 0.104 mmol), 1,8-diazabicyclo[5.4.0]-7-undecene (DBU) (15.5 μL, 0.104 mmol), and $Zn(OAc)_2$ (4.76 mg, 25.9 μmol) in 1-pentanol (1.0 mL) was stirred at 140 °C for 12 h under an Ar atmosphere. After cooling to rt, the reaction mixture was poured into H_2O and extracted with CH_2Cl_2 (3× 30 mL). The organic layer was washed with H_2O (3×50 mL), dried over Na_2SO_4, and the solvent evaporated. The residue was purified by column chromatography on activated alumina by eluting with *n*-hexane and recycling preparative HPLC, to give **ZnTNc$_{endo}$** as a dark green solid (51.8 mg, 51%); ^{1}H NMR ($CDCl_3$, 400.13 MHz): δ = 9.33 (8H, brs, Ar*H*), 2.79–3.53 (32H, br, CH_2), 1.28–2.09 (320H, br, CH_2), 0.82–0.89 ppm (48H, br, CH_3); UV/Vis-NIR (THF): λ (log ε/$M^{-1}cm^{-1}$) = 363 (5.13), 452 (4.83), 692 (4.84), 740 (4.83), 775 nm (5.57); MALDI-TOF MS (dithranol) *m*/*z* $[M+H]^+$ calcd for $C_{256}H_{408}N_8S_8Zn$: 3914.92, found 3914.91.

ZnTNc$_{exo}$: **ZnTNc$_{exo}$** was synthesized from **7** (80 mg, 83.0 μmol), DBU (12.4 μL, 20.8 μmol), and $Zn(OAc)_2$ (3.81 mg, 83.0 μmol) by the same procedure as for **ZnTNc$_{endo}$** to yield a dark green solid (41.0 mg, 50%); ^{1}H NMR ($CDCl_3$, 400.13 MHz): δ = 10.86 (8H, brs, Ar*H*), 2.51–4.41 (32H, br, CH_2), 0.48–2.34 ppm (368H, br, CH_2, CH_3); UV/Vis-NIR (THF): λ (log ε/$M^{-1}cm^{-1}$) = 353 (5.24), 475 (4.26), 692 (4.85), 739 (4.81), 778 nm (5.55); MALDI-TOF MS (dithranol) *m*/*z* $[M+H]^+$ calcd for $C_{256}H_{408}N_8S_8Zn$: 3914.92, found: 3914.44.

Time-of-flight measurements[52,53]

Measurement cells for TOF were composed of two Indium tin oxide (ITO) patterned glass substrates and a silicon spacer containing silica beads with 15 μm diameter. The effective area of the cells was 0.25 cm^2. Powdered samples of **ZnTNc$_{endo}$** or **ZnTNc$_{exo}$** (~5 mg)

were put on the bottom ITO substrate, and the cells placed in a vacuum oven. After evacuation, the oven was filled with Ar and heated at 210 or 260 °C for **ZnTNc$_{exo}$** and **ZnTNc$_{end}$**, respectively. The area between the two ITO electrodes was filled with melted **ZnTNc$_{exo}$** or **ZnTNc$_{endo}$** by injection from the cell slit through capillary action, and the cell was then cooled to rt at 1 °C min^{-1} inside the oven, to achieve the formation of large-area domains. The transient photocurrents were detected using a digital oscilloscope after light irradiation with a 377 nm N_2-pulse laser having a pulse width of 800 ps under various electric fields. An electric field was created in the cell using a DC power supply. The temperature of the cells was controlled within 0.2 K using a temperature controller and a hot stage. Carrier (hole or electron) mobility μ was calculated from the following equation, $\mu = d^2/(V t_t)$ where d is the sample thickness, V is the applied bias, and t_t is the transit time of the photo-generated carriers traversing the sample layer. The t_t values of the photo-generated carriers in the material were determined from an inflection point on the double logarithmic plot of the transient photocurrent decay curves.

Acknowledgements

This work was partially supported by Grant-in-Aid (No. 15H02172 to M. K. and N. K.) from the Ministry of Education, Culture, Sports, Science, and Technology (MEXT), Japan.

Keywords: carrier mobility · charge transport · columnar stacking · dyes/pigments · liquid crystalline · phthalocyanines

[1] A. J. Berresheim, M. Müller, K. Müllen, *Chem. Rev.* **1999**, *99*, 1747 – 1786.
[2] J. Wu, W. Pisula, K. Müllen, *Chem. Rev.* **2007**, *107*, 718 – 747.
[3] C. Li, M. Liu, N. G. Pshirer, M. Brumgarten, K. Müllen, *Chem. Rev.* **2010**, *110*, 6817 – 6855.
[4] S. Laschat, A. Baro, N. Steinke, F. Giesselmann, C. Hägele, G. Scalia, R. Judele, E. Kapatsina, S. Sauer, A. Schreivogel, M. Tosoni, *Angew. Chem. Int. Ed.* **2007**, *46*, 4832 – 4887; *Angew. Chem.* **2007**, *119*, 4916 – 4973.
[5] S. Kumar, *Chem. Soc. Rev.* **2006**, *35*, 83 – 109.
[6] C. G. Claessens, U. Hahn, T. Torres, *Chem. Rec.* **2008**, *8*, 75 – 97.
[7] K. M. Kadish, K. M. Smith, R. Guilard, *The Porphyrin Handbook, Vol. 15 – 20*, Academic Press, San Diego, CA, **2003**.
[8] C. Piechocki, J. Simon, A. Skoulios, D. Guillon, P. Weber, *J. Am. Chem. Soc.* **1982**, *104*, 5245 – 5247.
[9] O. A. Melville, B. H. Lessard, T. P. Bender, *ACS Appl. Mater. Interfaces* **2015**, *7*, 13105 – 13118.
[10] Q. Duy Dao, T. Hori, K. Fukumura, T. Masuda, T. Kamikado, A. Fujii, Y. Shimizu, M. Ozaki, *Appl. Phys. Lett.* **2012**, *101*, 263301.
[11] N. Kobayashi, S. Nakajima, H. Ogata, T. Fukuda, *Chem. Eur. J.* **2004**, *10*, 6294 – 6312.
[12] J. M. Fox, T. J. Katz, S. V. Elshocht, T. Verbiest, M. Kauranen, A. Persoons, T. Thongpanchang, T. Krauss, L. Brus, *J. Am. Chem. Soc.* **1999**, *121*, 3453 – 3459.
[13] E. M. Maya, A. W. Snow, J. S. Shirk, S. R. Flom, R. G. S. Pong, J. H. Callahan, *J. Porphyrins Phthalocyanines* **2002**, *6*, 463 – 475.
[14] T. Sooksimuang, B. K. Mandal, *J. Org. Chem.* **2003**, *68*, 652 – 655.
[15] L. X. Chen, G. B. Shaw, D. M. Tiede, X. Zuo, P. Zapol, P. C. Redfern, L. A. Curtiss, T. Sooksimuang, B. K. Mandal, *J. Phys. Chem. B* **2005**, *109*, 16598 – 16609.
[16] A. N. Cammidge, H. Gopee, *Chem. Eur. J.* **2006**, *12*, 8609 – 8613.
[17] Y. Fogel, M. Kastler, Z. Wang, D. Andrienko, G. J. Bodwell, K. Müllen, *J. Am. Chem. Soc.* **2007**, *129*, 11743 – 11749.
[18] L. Zöphel, K. S. Mail, P. S. Reddy, M. Wagner, S. De Feyter, W. Pisula, K. Müllen, *Chem. Eur. J.* **2012**, *18*, 3264 – 3276.
[19] D. K. P. Ng, Y.-O. Yeung, W. K. Chan, S.-C. Yu, *Tetrahedron Lett.* **1997**, *38*, 6701 – 6704.
[20] A. N. Cammidge, H. Gopee, *Chem. Commun.* **2002**, 966 – 967.
[21] Y. Zhang, N. Pan, Q. Xue, M. Bai, J. Jiang, *J. Porphyrins Phthalocyanines* **2006**, *10*, 1132 – 1139.
[22] M. Ichihara, M. Miida, B. Mohr, K. Ohta, *J. Porphyrins Phthalocyanines* **2006**, *10*, 1145 – 1155.
[23] C. Wang, H. Dong, W. Hu, Y. Liu, D. Zhu, *Chem. Rev.* **2012**, *112*, 2208 – 2267.
[24] M. E. Cinar, T. Ozturk, *Chem. Rev.* **2015**, *115*, 3036 – 3140.
[25] X. Yan, H. Fan, H. Gu, J. Zhang, X. Huang, R. Zhang, X. Zhan, *Dyes Pigm.* **2015**, *114*, 124 – 128.
[26] C.-Y. Kuo, W. Nie, H. Tsai, H.-J. Yen, A. D. Mohite, G. Gupta, A. M. Dattelbaum, D. J. William, K. C. Cha, Y. Yang, L. Wang, H.-L. Wang, *Macromolecules* **2014**, *47*, 1008 – 1020.
[27] T. Muroga, T. Sakaguchi, T. Hashimoto, *Polymer* **2012**, *53*, 4380 – 4387.
[28] J. L. Brusso, O. D. Hirst, A. Dadvand, S. Ganesan, F. Cicoira, C. M. Robertson, T. Oakley, F. Rosei, D. F. Perepichka, *Chem. Mater.* **2008**, *20*, 2484 – 2494.
[29] Q. Xiao, T. Sakurai, T. Fukino, K. Akaike, Y. Honsho, A. Saeki, S. Seki, M. Tanaka, T. Aida, *J. Am. Chem. Soc.* **2013**, *135*, 18268 – 18271.
[30] T. Ishiyama, M. Murata, N. Miyaura, *J. Org. Chem.* **1995**, *60*, 7508 – 7510.
[31] P. Sonar, S. P. Singh, P. Lecler, M. Surin, R. Lazzaroni, T. T. Lin, A. Dodabalapur, A. Sellinger, *J. Mater. Chem.* **2009**, *19*, 3228 – 3237.
[32] R. Martin, S. L. Buchwald, *Acc. Chem. Res.* **2008**, *41*, 1461 – 1473.
[33] V. G. Nenajdenko, E. S. Balenkova, K. Y. Chernichenko, S. S. Vshivenko, *Russ. Chem. Bull. Int. Ed.* **2012**, *61*, 1456 – 1462.
[34] D. Wöhrle, G. Schnurpfeil, G. Knothe, *Dyes Pigm.* **1992**, *18*, 91 – 102.
[35] K.-W. Poon, W. Liu, P.-K. Chan, Q. Yang, T.-W. D. Chan, T. C. W. Mak, D. K. P. Ng, *J. Org. Chem.* **2001**, *66*, 1553 – 1559.
[36] E. Maligaspe, T. Kumpulainen, H. Lemmetyinen, N. V. Tkachenko, N. K. Subbaiyan, M. E. Zandler, F. D'Souza, *J. Phys. Chem. A* **2010**, *114*, 268 – 277.
[37] E. Orti, M. C. Piqueras, R. Crespo, J. L. Brédas, *Chem. Mater.* **1990**, *2*, 110 – 116.
[38] B. Tieke, *Adv. Mater.* **1990**, *2*, 222 – 231.
[39] R. Zniber, R. Achour, M. Z. Cherkaoui, B. Donnio, L. Gehringer, D. Guillon, *J. Mater. Chem.* **2002**, *12*, 2208 – 2213.
[40] T. Sakurai, K. Shi, H. Sato, K. Tashiro, A. Osuka, A. Saeki, S. Seki, S. Tagawa, S. Sasaki, H. Masunaga, K. Osaka, M. Takata, T. Aida, *J. Am. Chem. Soc.* **2008**, *130*, 13812 – 13813.
[41] K. Ohta, S. Azumane, W. Kawahara, N. Kobayashi, I. Yamamoto, *J. Mater. Chem.* **1999**, *9*, 2313 – 2320.
[42] A. W. Snow in *The Porphyrin Handbook, Vol. 17* (Ed.: K. M. Kadish, K. M. Smith, R. Guilard), Academic Press, San Diego, CA, **2003**, *chap. 108*, pp. 129 – 176.
[43] H. Iino, J. Hanna, R. J. Bushby, B. Movaghar, B. J. Whitaker, M. J. Cook, *Appl. Phys. Lett.* **2005**, *87*, 132102.
[44] Y. Miyake, Y. Shiraiwa, K. Okada, H. Monobe, T. Hori, N. Yamasaki, H. Yoshida, M. J. Cook, A. Fujii, M. Ozaki, Y. Shimizu, *Appl. Phys. Express* **2011**, *4*, 021604.
[45] D. J. Tate, R. Anémian, R. J. Bushby, S. Nanan, S. L. Warriner, B. J. Whitaker, *Beilstein J. Org. Chem.* **2012**, *8*, 120 – 128.
[46] Z.-Y. Liu, T. Usui, H. Iino, J. Hanna, *J. Mater. Chem. C* **2013**, *1*, 8186 – 8193.
[47] H. Eichhorn, *J. Porphyrins Phthalocyanines* **2000**, *4*, 88 – 102.
[48] J. M. Warman, J. E. Kroeze, P. G. Schouten, A. M. van de Craats, *J. Porphyrins Phthalocyanines* **2003**, *7*, 342 – 350.
[49] R. J. Bushby, O. R. Lozman, *Curr. Opin. Solid State Mater. Sci.* **2002**, *6*, 569 – 578.
[50] W. Pisula, M. Zorn, J. Y. Chang, K. Müllen, R. Zentel, *Macromol. Rapid Commun.* **2009**, *30*, 1179 – 1202.
[51] A. M. van de Craats, J. M. Warman, *Adv. Mater.* **2001**, *13*, 130 – 133.
[52] H. Scher, E. W. Montroll, *Phys. Rev. B* **1975**, *12*, 2455 – 2477.
[53] H. Hayashi, W. Nihashi, T. Umeyama, Y. Matano, S. Seki, Y. Shimizu, H. Imahori, *J. Am. Chem. Soc.* **2011**, *133*, 10736 – 10739.

Received: November 9, 2015
Published online on November 24, 2015

